Using polynomial optimization to solve the fuel-optimal impulsive rendezvous problem

Denis Arzelier[1], Mounir Kara-Zaitri[2], Christophe Louembet[3]

CNRS ; LAAS ; 7 avenue du colonel Roche, F-31077 Toulouse, France

Université de Toulouse ; UPS, INSA, INP, ISAE ; LAAS ; F-31077 Toulouse, France

Akin Delibasi[4]
Department of Electrical Engineering, Yıldız Technical University, Beşiktaş, Istanbul, Turkey

The optimal fuel impulsive time-fixed rendezvous problem is reviewed. In a linear setting, it may be reformulated as a nonconvex polynomial optimization problem for a pre-specified fixed number of velocity increments. A numerical algorithm using a convex relaxation based on a sum-of-squares representation of positive polynomials is first proposed. Its numerical efficiency is assessed using a classical example from the literature. Relying on variational results previously published in the literature, an improved mixed iterative algorithm is defined to address the issue of optimization over the number of impulses. Revisiting the primer vector theory, it combines variational tests with sophisticated numerical tools from algebraic geometry to solve polynomial necessary and sufficient conditions of optimality. Even if in this paper, relative motion is modelled by the transition matrix for elliptic Keplerian orbits, this algorithm can also be used for any transition matrix of relative motion. Numerical examples under circular and elliptic assumptions show that both algorithms are complementary and can be integrated into a single rendezvous planning tool.

[1] Directeur de Recherche CNRS, LAAS-CNRS, Methods and Algorithms in Control, arzelier@laas.fr
[2] Ph.D. student, LAAS-CNRS, Methods and Algorithms in Control, kara-zaitri@laas.fr
[3] Associate Professor, LAAS-CNRS, Methods and Algorithms in Control, louembet@laas.fr
[4] Postdoctoral Research fellow, CNRS, LAAS-CNRS, Methods and Algorithms in Control, adelibas@laas.fr

Nomenclature

- a = semi-major axis ;

- e = eccentricity ;

- ν = true anomaly ;

- $\phi^{\#'}(\nu) = \phi^{-1}(\nu)$ and $\phi(\nu)$ = fundamental matrix of relative motion ;

- $\Phi(\nu, \nu_1) = \phi(\nu)\phi^{-1}(\nu_1)$ = transition matrix of relative motion ;

- $B(\nu)$ = input matrix of relative motion dynamical model ;

- $R(\nu) = \phi^{\#t}(\nu)B(\nu) = \phi^{-1}(\nu)B(\nu)$ = primer vector evolution matrix ;

- $u_f = \phi^{-1}(\nu_f)X_f - \phi^{-1}(\nu_1)X_1 \neq 0$ = boundary conditions ;

- N = number of velocity increments ;

- $\nu_i, \forall\, i = 1, \cdots, N$ = impulses application times ;

- Δv_i = impulse modulus at ν_i ;

- $\beta(\nu_i)$ = impulse direction vector at ν_i ;

- $\Delta V(\nu_i) = \Delta v_i \beta(\nu_i)$ = velocity increment vector at ν_i ;

- $\mathbb{R}[x_1, \cdots, x_n]$ stands for the algebra of polynomials in variables $(x_1, \cdots, x_n)$ with coefficients in $\mathbb{R}$;

I. Introduction

The first space missions involving more than one vehicle (Gemini, Apollo, Vostok) have highlighted the fact that the space rendezvous between two spacecraft is a key technology raising relevant open control issues. Given the increasing need for satellite servicing in current and future space programs developed in conjunction with rendezvous missions for the International Space Station (ISS), the interest of most space agencies in the Guidance Navigation and Control (GNC) systems has been rapidly rising. In particular, new challenges have appeared relating to the synthesis of guidance schemes capable of achieving autonomous far range rendezvous on highly elliptical orbits while preserving optimality in terms of fuel consumption.

Strictly speaking, the space rendezvous maneuver is an orbital transfer between a passive target and an actuated spacecraft called the chaser, within a fixed or floating time period. Since the rendezvous maneuver can only be performed within a certain period of time while utilizing as little fuel as possible to extend the chaser lifetime, we mainly focus on the so-called time-fixed fuel optimal rendezvous problem [1], [2], [3].

In this paper, far range rendezvous in a linearized gravitational field is viewed as a time-fixed minimum-fuel impulsive orbital transfer between two known elliptical orbits. This issue may therefore be formulated as a time-fixed impulsive optimal control problem. Because of the constraints of on-board guidance algorithms, numerical solutions based on linear relative motion are particularly appealing. With respect to the numerical solution, direct methods based on discretizing the original problem and converting it into a linear programming problem may be used as in [4]. Indirect approaches based on the solution of optimality conditions derived from Pontryagin's Maximum Principle, leading to the development of the so-called primer vector theory presented in [5], have also been an avenue of research in numerous studies [6], [7], [2], [8]. If they only focus on fixed number and location of impulses, these approaches fail to optimize trajectory planning in terms of the number of impulsive maneuvers. Neither can they ensure the global optimality of the result provided for a fixed number of impulses. To optimize the number of impulses as well as their specific application times, an iterative algorithm based on the calculus of variations originally developed by Lion and Handelsman [9] has been designed [10–12]. The main drawback however is due to the possible non smoothness and sub-optimality of the resultant trajectory of the primer vector norm. To overcome this difficulty, a Davidon-Fletcher-Powell penalty minimization step is proposed in order to move the impulses and achieve a smooth trajectory as detailed in [11] or [1].

The paper's contribution is twofold: First, by exploiting the polynomial nature of the necessary and sufficient conditions of optimality of the time-fixed impulsive optimal control problem for a fixed number of impulses, a new powerful algorithm can be designed. Based on recent results on convex relaxations for non-linear polynomial optimization [13], [14], the first rendezvous algorithm can be devised with the use of time interval grid that helps find the optimal location of the impulsive maneuvers. One of the key advantages is to furnish a certificate of global optimality for the proposed solution. Secondly, the iterative algorithm based on the calculus of variations is revisited and extended to the case of elliptic Keplerian orbits. In particular, this new iterative algorithm combines the algebraic formulation of Carter's necessary and sufficient conditions,

supporting the use of powerful numerical tools from the algebraic geometry field, and improving variational tests as derived in [9]. This results in a mixed different iterative strategy bypassing the local optimal search step and cusp occurrence. An interesting feature of the present results is that both algorithms complement each other and may be integrated into a single optimal trajectory planning tool.

In the first section of this paper, the framework of the minimum-fuel fixed-time rendezvous problem is presented and necessary and sufficient conditions of optimality are recalled. Relative dynamics motion for rendezvous are the well-known Tschauner-Hempel equations [15] and the transition matrix of Yamanaka-Ankersen [16]. It is shown that, under mild classical assumptions, the rendezvous problem may be reformulated as a polynomial optimization problem in which a first rendezvous algorithm based on polynomial optimization is designed for a number of impulses specified *a priori*. The results of [9] are recalled and the mixed iterative algorithm is presented. For comparison's sake, the efficiency of the proposed algorithms is illustrated with four different numerical examples. Two academic examples taken from Carter's reference [2] are first studied. Also reviewed are two realistic scenarios based on PRISMA which is a "technology in-orbit testbed mission" demonstrating formation flight [17] and SIMBOL-X formation flying mission which is a particular example of a high elliptical reference orbit [18].

II. The time-fixed optimal rendezvous problem as a polynomial optimization problem

A. Time-fixed optimal rendezvous problem in a linear setting

This paper focuses on transfers between closed non-circular orbits for the fixed-time minimum-fuel rendezvous of an active (actuated) spacecraft called the chaser with a passive target spacecraft assuming a linear impulsive setting and an unperturbed Keplerian relative motion. The impulsive approximation for the thrust means that instantaneous velocity increments are applied to the chaser instead of finite-thrust powered phases of finite duration. The thrust per unit mass vector is therefore defined by:

$$\Gamma(\nu) = \sum_{i=1}^{N} \Delta V(\nu_i)\delta(\nu - \nu_i) = \sum_{i=1}^{N} \Delta v_i \beta(\nu_i)\delta(\nu - \nu_i) \tag{1}$$

where $0 \leq \nu_1 \leq \cdots \leq \nu_N \leq T$, N is the number of impulsive controls and $\Delta V(\nu_i)$ the discontinuity in the velocity vector due to a thrust impulse at ν_i, defined by $\delta(\nu - \nu_i)$. Note that the true anomaly has been chosen as the independent variable since this change of variables is widely used when dealing with Tschauner-Hempel equations [15] and Yamanaka-Ankersen's state transition matrix [16]. For a minimum-

fuel rendezvous, the cost function is defined by the total characteristic velocity:

$$J = \int_0^{\nu_N} \Gamma(\nu) d\nu = \sum_{i=1}^{N} \Delta v_i \tag{2}$$

If the relative equations of motion of the chaser are supposed to be linear and under the previous assumptions, the considered rendezvous problem may be reformulated as the following optimal control problem:

$$\begin{aligned} \min_{N,\nu_i,\Delta v_i,\beta(\nu_i)} \quad & J = \sum_{i=1}^{N} \Delta v_i \\ \text{s.t.} \quad & \dot{X}(\nu) = A(\nu)X(\nu) + B(\nu)\sum_{i=1}^{N} \beta(\nu_i)\Delta v_i \delta(\nu - \nu_i) \\ & \|\beta(\nu_i)\| = 1 \\ & \Delta v_i \geq 0 \end{aligned} \tag{3}$$

where matrices $A(\nu)$ and $B(\nu)$ define the state-space model of relative dynamics. Recalling the Keplerian elliptic assumptions, the differential constraint in (3) is given by the Tschauner-Hempel (TH) equations [15]:

$$\dot{X}(t) = \begin{bmatrix} \delta\dot{r} \\ \\ \delta\dot{v} \end{bmatrix} = \begin{bmatrix} 0_n & I_n \\ \\ A_1(\nu) & A_2(\nu) \end{bmatrix} \begin{bmatrix} \delta r \\ \\ \delta\dot{r} \end{bmatrix} \tag{4}$$

where δr and δv are the relative position and velocity vectors respectively. $A_1(\nu)$ is a symmetric matrix and A_2 is a time-invariant antisymmetric matrix $A_2(\nu) = A_2 = -A_2^t$ while $B = \begin{bmatrix} \mathbf{0} & \mathbf{1} \end{bmatrix}'$. The optimal control problem (3) belongs to the class of impulsive linear control problems (see [19] and references therein) for which a numerical solution is hard to construct. One of the main difficulties encountered with problem (3) is that the number of impulses N is part of the optimization process. A highly classical relaxation of (3) consists of reviewing a fixed-scenario optimal rendezvous for which the number of impulses N is *a priori* set and where the first and last impulses are applied at the beginning and end of the rendezvous [6] respectively. It should be pointed out that the number of impulses N may be chosen equal to the upper-bound on the optimal number of impulses according to Neustadt [20] (that is 2 for out-of-plane rendezvous, 4 for a coplanar rendezvous and 6 for the complete rendezvous). Moreover, since a transition matrix may be computed in closed form for the TH equations (see [16]), it may be appropriate to replace the differential constraint on dynamics by the equivalent algebraic constraint involving this transition matrix. Assuming boundedness conditions on relative position and velocity, problem (3) for a fixed number of impulses N may

then be reformulated as the following optimization problem [8]:

$$\begin{aligned} \min_{\nu_i, \Delta v_i, \beta(\nu_i)} \quad & J = \sum_{i=1}^{N} \Delta v_i \\ \text{s.t.} \quad & u_f = \sum_{i=1}^{N} \phi^{\#'}(\nu_i) B(\nu_i) \Delta v_i \beta(\nu_i) = \sum_{i=1}^{N} R(\nu_i) \Delta v_i \beta(\nu_i) \\ & \|\beta(\nu_i)\| = 1 \\ & \Delta v_i \geq 0 \end{aligned} \tag{5}$$

where: $\phi^{\#'}(\nu) = \phi^{-1}(\nu)$ and $\phi(\nu)$ is the Yamanaka-Ankersen fundamental matrix for relative motion. The optimization decision variables are :

- $\nu_i, \forall\, i = 1, \cdots, N$: Impulses application times ;

- Δv_i: Impulse modulus at ν_i ;

- $\beta(\nu_i)$: Impulse direction vector at ν_i ;

B. Primer vector theory and Carter's necessary and sufficient conditions for a fixed number of impulses

Applying the Maximum Principle on problem (3) for a fixed number of impulses N as described in Lawden [5] or a Lagrange multiplier rule for the equivalent problem (5) as in [21], one can derive necessary conditions of optimality in terms of the co-state vector associated with the relative velocity and referred to as the primer vector (see conditions (6) to (10) in theorem II.1 below). Carter has shown that these conditions are also sufficient in the case of linear relative motion with the strengthening semi-infinite constraint (13) that should be fulfilled on the continuum $[\nu_1, \nu_N]$ and is expressed in terms of the transition matrix $R(\nu) = \phi^{\#'}(\nu)B(\nu) = \phi^{-1}(\nu)B(\nu)$ of the primer vector denoted $\lambda_v(\nu) = R(\nu)\lambda$. These results are summarized in the following theorem.

Theorem II.1 *[8]*

$(\nu_1, ..., \nu_N, \Delta v_1, ..., \Delta v_N, \beta(\nu_1), ..., \beta(\nu_N))$ *is the optimal solution of problem* (5) *if and only if there exists a non-zero vector* $\lambda \in \mathbb{R}^m,\ m = \dim(\phi)$ *that verifies the necessary and sufficient conditions:*

$$\Delta v_i = 0 \text{ or } \beta(\nu_i) = -R'(\nu_i)\lambda,\ \forall\, i = 1, \cdots, N = 2 + r \tag{6}$$

$$\Delta v_i = 0 \text{ or } \lambda' R(\nu_i) R(\nu_i)' \lambda = 1,\ \forall\, i = 1, \cdots, N \tag{7}$$

$$\Delta v_{k_i} = 0 \text{ or } \nu_{k_i} = \nu_1 \text{ or } \nu_{k_i} = \nu_f \text{ or } \lambda' \frac{dR(\nu_{k_i})}{d\nu} R(\nu_{k_i})'\lambda = 0,\ \forall\, i = 2, \cdots, N-1 \tag{8}$$

$$\sum_{i=1}^{N} \left[R(\nu_i)R'(\nu_i)\right] \lambda \Delta v_i = -u_f \tag{9}$$

$$\Delta v_i \geq 0,\ \forall\, i = 1, \cdots, N \tag{10}$$

$$\sum_{i=1}^{N} \Delta v_i = -u_f'\lambda > 0 \tag{11}$$

$$-u_f'\lambda \text{ is the minimum of the set defined as : } \{\lambda \in \mathbb{R}^m \ :\ (6)-(11) \text{ are verified}\} \tag{12}$$

$$\|\lambda_v(\nu)\| \leq 1 \ \ \forall\, \nu \in [\nu_1, \nu_f] \tag{13}$$

Note that conditions (11) and (12) may be easily derived from the previous ones.

Numerical solution of optimality conditions (6) to (13) in the unknowns $\lambda \in \mathbb{R}^m$, $\{\nu_i\}_{i=1,\cdots,N}$, $\{\beta_i\}_{i=1,\cdots,N}$, $\{\Delta v_i\}_{i=1,\cdots,N}$ is still hard to find for a fixed number of impulses N due to the nonconvex and transcendental nature of these polynomial equalities and inequalities. A numerical procedure based on polynomial optimization is now proposed to address this numerical issue and .

C. Numerical insights for the relaxed fixed-scenario optimal rendezvous

Despite the preceding simplifying assumptions, the fact that impulse dates are part of the vector of decision variables implies the solution of transcendental equations. This first difficulty may be overcome thru the use of a gridding technique providing a numerical approximation of the optimal impulse dates. The major drawback of gridding techniques is the definition of the resolution value (density) of grid points in order to adequately handle hard equality constraints as defined in (8). Therefore, we propose a dynamic gridding strategy to overcome the first drawback while equality constraints (8) are relaxed as:

$$-\epsilon_1 < \lambda' \frac{dR(\nu_{k_i})}{d\nu} R(\nu_{k_i})'\lambda < \epsilon_1,\ \forall\, i = 2, \cdots, N-1 \tag{14}$$

where $\epsilon_1 > 0$ is a small parameter representing the tolerance over equality constraints.

Furthermore, verifying (13) requires imposing the positivity of the quadratic polynomial $1 - \lambda' R(\nu)R(\nu)\lambda$ on the continuum of the whole rendezvous interval $[\nu_1, \nu_f]$. This inequality constraint is

not as hard as the previous ones and may be roughly discretized over a static grid of M_d equidistant points considering that a few number of points (typically 50) will be necessary to satisfy this constraint due to the usual shape of the function $\|\lambda_v\|$. In every case, the primer vector trajectory will be propagated and checked *a posteriori* on a finer grid of points.

Another issue is related to the poor scaled representation due to large differences between initial time and positions and final ones. One can easily see that (7) is already in a Cholesky factorized form and other conditions may be factorized using λ and Δv_i's decision variables. Therefore, the problem could be scaled using Schur decomposition. However, as the scaling matrix entries differ by several orders of magnitude in this case, a different scaling strategy has been preferred. First, diagonal temporary scaling matrices (S_{T_i}) are calculated for each impulse ($i = 1, \ldots, N$). The main purpose is to make diagonal entries of $Q_{S_i} = S_{T_i} R(t_i) R'(t_i) S_{T_i}$ matrix less than or equal to 1. Second, entries of diagonal scaling matrix (S) are defined using the corresponding entries of minimum value of S_{T_i} matrices.

Finally, the previous necessary and sufficient conditions show that the optimal directions $\beta(\nu_i)$ may easily be obtained via (6) once λ and Δv_i have been computed.

For a given grid of impulse times, the optimization problem is then given by:

$$
\begin{aligned}
&\min_{\lambda, \Delta v_i} \; -u_f' \lambda \\
&\text{s.t.} \\
&-u_f = \sum_{i=1}^{N} R(\nu_i) R'(\nu_i) S \lambda \Delta v_i \\
&\lambda' S R(\nu_i) R(\nu_i)' S \lambda = 1, \; \forall \, i = 1, \cdots N \\
&\left| \lambda' S \frac{dR(\nu)}{d\nu} R(\nu_i)' S \lambda \right| < \epsilon, \; \forall \, i = 2, \cdots, N-1 \\
&\Delta v_i \geq 0, \; \forall \, i = 1, \cdots N \\
&\lambda' S R(\nu_j) R(\nu_j)' S \lambda \leq 1, \; \forall \, j = 0, \cdots, M_d
\end{aligned}
\tag{15}
$$

The problem (15) belongs to the class of polynomial nonconvex optimization problems with respect to the variables $\lambda \in R^m$ and Δv_i, $i = 1, ..., N$ for which a hierarchy of convex relaxations has been proposed [13], [14]. Given below in the next section are some basic facts about convex relaxations of nonconvex polynomial optimization problems.

D. Convex relaxations for polynomial optimization

The problem (15) can be written under the general form:

$$\begin{aligned} \mathbb{P}: \; g^\star \; &= \; \min \;\; g_0(x) \\ &\text{s.t.} \quad g_i(x) \geq 0, \; i = 1, \ldots, l \end{aligned} \tag{16}$$

where $g_i(x) \in \mathbb{R}[x_1, \cdots, x_n] \; : \; \mathbb{R}^n \to \mathbb{R}$. This class of optimization problems is known as NP-hard. The quadratic non convex problems (0-1 problems) are particular cases of (16). The feasible set of (16) is noted:

$$\mathbb{K} = \{x \in \mathbb{R}^n \mid g_i \geq 0, \; i = 1, \ldots, m\} \tag{17}$$

Computing the global optimum of $\mathbb{P}$ is effected by finding g^*, where $g_0(x) - g^\star \geq 0$ is a globally positive polynomial on the set $\mathbb{K}$ i.e. $g_0(x) - g^\star \in \mathcal{P}_n^d$, the convex cone of semi definite positive polynomials (SDP) in $\mathbb{R}^D$ having degree $\leq d$ defined by:

$$\mathcal{P}_n^d = \{p \in \mathbb{R}[x_1, \cdots, x_n] \mid p(x) \geq 0 \; \forall \; x \in \mathbb{R}^n\} \qquad D = \begin{pmatrix} n+d \\ \\ d \end{pmatrix} \tag{18}$$

If $\mathcal{S}_n^d$ is the convex cone of sum of squares polynomials (SOS) in $\mathbb{R}^D$ given by:

$$\mathcal{S}_n^d = \left\{ p \in \mathbb{R}[x_1, \cdots, x_n] \mid p(x) = \sum_{i=1}^{r} q_i(x)^2 \right\} \tag{19}$$

then each element of $\mathcal{S}_n^d$ can be characterized by a linear matrix inequality (LMI) formulation [14], [13], [22]:

$$p(x) = \sum_{\alpha} p_\alpha x^\alpha \in \mathcal{S}_n^d \;\; \Leftrightarrow \;\; \exists \, X \; : \; p(x) = z' X z \quad X \succeq 0 \tag{20}$$

where z is the monomials of degrees $\leq d$ array. For a feasible matrix X, Cholesky factorization gives:

$$X = Q'Q \;\; Q' = \left[\; q_1, \; \cdots \; , q_r \; \right] \tag{21}$$

and

$$p(x) \; = \; z'Q'Qz = \|Qz\|_2 = \sum_{i=1}^{r} (q_i' z)^2 = \sum_{i=1}^{r} q_i^2(x) \tag{22}$$

where the number of squared terms is r = $\operatorname{rang}(X)$. By identifying the coefficients of $p(x) = z'Xz = \sum_\alpha p_\alpha x^\alpha \geq 0$, we obtain the following LMIs:

$$\begin{aligned} &\operatorname{trace} H_\alpha X = p_\alpha \quad \forall \, \alpha \\ &X \succeq 0 \end{aligned} \tag{23}$$

where H_α is a Hankel matrix. Determining whether a polynomial belongs to $\mathcal{S}_n^d$ is therefore equivalent to solving an LMI problem where powerful solvers may be used [23]. Furthermore, $\mathcal{S}_n^d \subset \mathcal{P}_n^d$: A lower bound to the polynomial optimization problem (16) may be easily computed. Finding the multipliers $q_i(x) \in \mathcal{S}_n^d$ such that:

$$p(x) \;=\; g_0(x) - g^* = q_0(x) + \sum_{i=1}^{m} g_i(x) q_i(x) \Rightarrow g_0(x) - g^* \geq 0 \;\; \forall\, x \in \mathbb{K} \tag{24}$$

for a fixed $\deg(q_i(x))$, is a semi-definite programming problem. For $\deg(p(x)) = 2k$, the k^{th} order convex LMI relation stating that $p(x) = g_0(x) - g^* \in \mathcal{S}_n^d,\ \forall\, x \in \mathbb{K}$ is an LMI problem whose optimal solution $p_k^\star$ gives a lower bound to the global optimum g^*. Under some assumptions, it has been shown in [13] that a hierarchy of monotone convex relaxations can be constructed which asymptotically converges to the global optimum of the problem (16).

Theorem II.2 *[13]*

If $\mathbb{P}$ is compact and if there exists $u(x) \in \mathbb{R}[x_1, \cdots, x_n]$ such that:

$$1 -\ \{u(x) \geq 0\} \text{ is compact}$$
$$2 -\ u(x) = u_0(x) + \sum_{i=1}^{m} g_i(x) u_i(x) \;\; \forall\, x \in \mathbb{R}^n \text{ where } u_i(x) \in \mathcal{S}_n^l,\ i = 0, \cdots, m$$

then $p_k^\star \leq g^\star$ with an asymptotical convergence guarantee $\lim_{k \to \infty} p_k^\star = g^\star$.

Usually, convergence is fast and $p_k^\star$ tends to be extremely close to $g^\star$ for a low relaxation order k. If $p_k^\star = g^*$ for a given relaxation order k, a certificate of global optimality may be provided [22].

III. Using a polynomial optimization algorithm to solve the rendezvous problem

In this section, the complete rendezvous algorithm is presented. It relies on the dynamic gridding strategy and relaxations of the genuine polynomial optimization problem as detailed in the preceding section. Algorithm input arguments are the initial state (position/velocity) X_1, the final state vector X_f, the desired resolution (res_d) on the impulse times, dimension of Θ_i sets (d), first impulse time (ν_1), final impulse time (ν_f), number of impulses (N), initial precision value ϵ_1 for (14) and precision value ϵ_2 on the norm of the primer vector. The output arguments are the optimum impulse times ($\nu_2^\star, \ldots, \nu_{N-1}^\star$), optimal primer vector λ^*, optimal impulses (optimal amplitude Δv_i^* and optimal direction β_i^*) and the optimal fuel consumption J^*.

Let $\Theta_2, \ldots, \Theta_{N-1}$ be nonempty ordered sets given by $\Theta_i := \{\nu_{i_1}, \ldots, \nu_{i_d}\}$ where $\nu_{i_1}, \ldots, \nu_{i_d}$ represent the possible candidates for i^{th} impulse time. The distances between sequential candidates are equal and represented by the current resolution value (res). In addition to these $N-2$ sets, it is necessary to define the two singletons $\Theta_1 = \{\nu_1\}$ and $\Theta_N = \{\nu_f\}$.

A. PRDV algorithm

1 Let $\nu_{i_1} := \nu_1$, $\nu_{i_d} := t_f$ for all $i = 2, \cdots, N-1$.

2 Generate all Θ_i sets for all $i = 2, \ldots, N-1$.

3 Generate the set $\mathcal{S}$ consisting of all the grid vectors of impulses dates:

$$\mathcal{S} := \left\{ \begin{bmatrix} \nu_1 & x_2 & \cdots & x_{N-1} & \nu_f \end{bmatrix}^t \in \mathrm{R}^N : x_i \in \Theta_i, \;\; x_i < x_{i+1}, \forall i = 2, \ldots, N-1 \right\} \tag{25}$$

4 Compute the global optimal solution α_k, $k = 1, \cdots, \mathrm{card}(\mathcal{S})$, if it exists, of the polynomial optimization problem (15) for every grid vector in $\mathcal{S}$.

5 If there exists no global solution α_i, let $\epsilon_1 \leftarrow \epsilon_1 + \frac{\epsilon_1}{2}$ and go to previous step.

6 Find the best solution $\alpha^* = \min_i \alpha_i$ and its argument (optimal grid vector $[\nu_1, x_2^\star, \ldots, x_{N-1}^\star, \nu_f]^t$ in $\mathcal{S}$ set, optimal amplitudes Δv_i^*, $i = 1, \cdots, N$, optimal costate vector λ^*) w.r.t. fuel consumption.

7 Define $l_i := \{x_i \in \Theta_i : x_i < x_i^\star\}$ and $u_i := \{x_i \in \Theta_i : x_i > x_i^\star\}$ sets for all $i = 2, \ldots, N-1$.

8 Calculate the resolution value ($res = \nu_{2_2} - \nu_{2_1}$).

9 If the l_i set is nonempty then assign $\nu_{i_1} \leftarrow \max(l_i)$ else $\nu_{i_1} \leftarrow x_i^\star$.

10 If the u_i set is nonempty then assign $\nu_{i_d} \leftarrow \min(u_i)$ else $\nu_{i_d} \leftarrow x_i^\star$.

11 If the resolution value is greater than res_d, let $\epsilon_1 \leftarrow \frac{\epsilon_1}{2}$ and go to Step 2 else go to step 12.

12 Check the primer vector with $(\lambda^*, (\Delta v_i^*)_{i=1,\cdots,N}, (\nu_i^*)_{i=1,\cdots,N})$

$$\|R'(\nu)\lambda\|_2 - 1 \leq \epsilon_2 \tag{26}$$

13 If the previous test is positive, compute the directions and amplitude of the optimal impulses:

$$\beta^*(\nu_i^*) = -R(\nu_i^*)'\lambda^* \quad \Delta V^*(\nu_i^*) = \beta^*(\nu_i^*)\Delta v_i^* \tag{27}$$

Some additional comments are now given for a greater clarity of each step.

- Polynomial optimization is achieved under MATLAB©, using the free academic Gloptipoly software developed at LAAS [22]. This software package requires the use of YALMIP [24] and SeDuMi [23].
- The 12^{th} step is carried out by propagating the primer vector initial condition λ^* over the rendezvous time duration using the Yamanaka-Ankersen transition matrix.
- Each optimal solution obtained at 4^{th} step for each grid point is certified to be global if it exists.

B. Numerical illustration

Consider the first example presented by Carter in [2]. It consists of a coplanar four-impulse circle-to-circle rendezvous. The rendezvous maneuver must be completed in one orbital period. Initial and final state vectors are given in table 1.

Eccentricity	$e = 0$
ν_0	0 rad
$X_0^t = [R_0^t \; v_0^t]$	$[\,1 \;\; 0 \;\; 0 \;\; 0\,]$
ν_f	2π rad
$X_f^t = [R_f^t \; v_f^t]$	$[\,0 \;\; 0 \;\; 0 \;\; 0.427\,]$
N_{max}	4

Table 1: Data for Carter's first example

Running the PRDV algorithm with $res_d := 5.1906 \times 10^{-4}$ rad (0.5 s), $d := 18$ and $\epsilon_1 := 5 \times 10^{-4}$, the global optimal solution can be found with an acceptable tolerance value ($\epsilon_1 = 4.4349 \cdot 10^{-7}$). For the sake of comparison, the results are shown in Table 2 (absolute precision less than 0.01 for the dates of application of velocity increments) alongside those of reference [2].

	Carter [2]	PRDV Algorithm
λ^*	$\begin{bmatrix} -9.8201 \cdot 10^{-2} \\ -5.2929 \cdot 10^{-2} \\ 1.8228 \cdot 10^{-1} \\ -4.3629 \cdot 10^{-1} \end{bmatrix}$	$\begin{bmatrix} -6.5876 \cdot 10^{-2} \\ -6.4727 \cdot 10^{-1} \\ 2.53 \cdot 10^{-4} \\ -6.2193 \cdot 10^{-1} \end{bmatrix}$
ν_{int_1} (rad)	$\frac{\pi}{2} \simeq 1.57$	1.7077
ν_{int_2} (rad)	$\frac{3\pi}{2} \simeq 4.7124$	4.5859
$\Delta V(\nu_0)^t$	$[\ -0.0273 \quad 0.0344\ ]$	$[\ -0.02655 \quad 0.0329\ ]$
$\Delta V(\nu_1)^t$	$[\ 0.0897 \quad 0.0119\ ]$	$[\ 0.0917 \quad 0.004614\ ]$
$\Delta V(\nu_2)^t$	$[\ -0.0897 \quad 0.0119\ ]$	$[\ -0.09011 \quad 0.00434\ ]$
$\Delta V(\nu_f)^t$	$[\ 0.0273 \quad 0.0344\ ]$	$[\ 0.0259 \quad 0.0322\ ]$
Fuel-cost $\mathcal{L}_1$ m/s	0.3230	0.3091
Fuel-cost $\mathcal{L}_2$ m/s	0.2688	0.2667

Table 2: Result comparison for Carter's first example

Interestingly, the results are not so different due to Carter's particularly smart *a priori* choice of the impulsive dates. Nevertheless, Carter's results are clearly not optimal.

More details about Carter's solution and PRDV solution are given in the plot of the in-plane trajectories of both solutions shown in Fig. 1 where red stars depict the positions of the application of the velocity increments. If these solutions lead to almost similar trajectories and consumption, only the one obtained with the PRDV algorithm is guaranteed to be optimal for the fixed number of impulses $N = 4$.

The main shortcoming here is that N, the velocity increment number is considered fixed and cannot be optimized except by running PRDV algorithm for each different case $N = 3,\ N = 4,\ \cdots$ up to the theoretical maximum defined by the Neustadt bound. An alternative to this gridding approach allowing optimization over the number of impulses dates back to the sixties with the seminal results of Lion-Handelsman [9] and the extensions reported in [12], [10], [25], [11]. This approach is now revisited and a new mixed iterative algorithm relying on the calculus of variations of Lion-Handelsman and on the polynomial solution of some part of the optimality conditions as formulated by Carter is built.

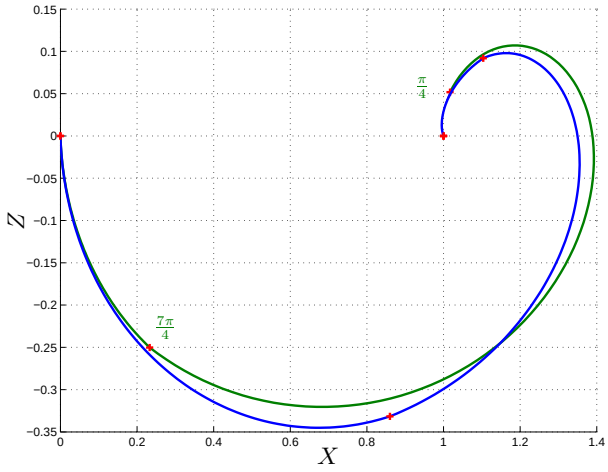

Figure 1: Detailed trajectories for solutions: PRDV algorithm (blue), Carter's solution (green)

IV. Optimizing over the number of impulses

A. Lion & Handelsman [9] results revisited

In [9], a method is proposed to take advantage of the primer vector theory developed by Lawden in order to improve nonoptimal trajectories by adding or shifting impulses. The calculus of variations is used to find conditions on the norm of the primer vector for an additional impulse and on the derivative of this norm for initial and/or final coastings. The method is mainly based on derivation of the so-called *variational adjoint equation* resulting from the variation of the cost function. Later, Jezewski [12], [10], [25], [11] developed a numerical algorithm combining Lion-Handelsman's conditions with a modified gradient search approach in a linear model setting. The additional local optimization procedure is used to find the optimal position and modulus of the additional impulse so as to avoid a resulting cusp for the norm of the primer vector as reported in [10]. In this section, these results are recalled, extended to the Tschauner-Hempel [15] dynamical relative model for elliptical reference orbit and a slightly different iterative procedure avoiding local optimal search step and cusp occurrence is proposed.

1. Variational adjoint equation

Recall the relative motion equation given by (4). The Hamiltonian associated with the optimal control problem (3) is defined by the relation:

$$H = \lambda_r^t \delta\dot{r} + \lambda_v^t \delta\dot{v} \tag{28}$$

where $\begin{bmatrix} \lambda_r \\ \\ \lambda_v \end{bmatrix}$ is the costate vector. Using Pontryagin's maximum principle and writing down the canonical Hamiltonian equations, one can add to (4) the dynamical equation for the costate vector:

$$\begin{bmatrix} \dot{\lambda}_r \\ \\ \dot{\lambda}_v \end{bmatrix} = - \begin{bmatrix} 0_n & I_n \\ \\ A_1 & A_2 \end{bmatrix}^t \begin{bmatrix} \lambda_r \\ \\ \lambda_v \end{bmatrix} = \begin{bmatrix} 0_n & -A_1 \\ \\ -I_n & A_2 \end{bmatrix} \begin{bmatrix} \lambda_r \\ \\ \lambda_v \end{bmatrix} \tag{29}$$

From Eqs. (29) and (4), one gets:

$$\ddot{\lambda}_v = A_1 \lambda_v + A_2 \dot{\lambda}_v \tag{30}$$

$$\ddot{\delta} r = A_1 \delta r + A_2 \delta v \tag{31}$$

(30)$\times \delta r^t -$ (31)$\times \lambda_v^t$ yields:

$$\lambda_v^t \ddot{\delta} r - \delta r^t \ddot{\lambda}_v = 0 \tag{32}$$

Adding and subtracting $\dot{\lambda}_v^t \delta v$, the following relation is obtained:

$$\lambda_v^t \ddot{\delta} r + \dot{\lambda}_v^t \delta v - \delta r^t \ddot{\lambda}_v - \dot{\lambda}_v^t \delta v = 0 \Leftrightarrow \frac{d}{dt} \left\{ \lambda_v^t \delta v - \dot{\lambda}_v^t \delta r \right\} = 0 \tag{33}$$

In other words:

$$\lambda_v^t \delta v - \dot{\lambda}_v^t \delta r = \text{constant} \tag{34}$$

Equation (34) is known as the *variational adjoint equation* [26]. Lion-Handelsman's idea is to compute variations of the cost function and to derive different conditions on the primer vector that will lead to a reduction of the cost thanks to the variational adjoint equation. The complete derivation of these conditions based on the calculus of variations may be found in [10] (see also [27] for more recent information) in the case of variations related to the addition of (i) an interior impulse for a two-impulse reference trajectory and (ii) an initial and/or final coasting period. These conditions are now recalled for the different cases.

2. Additional interior impulse condition

Perturbing a reference initial two-impulse trajectory and adding an interior impulse at t_m, the differential cost can be expressed as:

$$\delta J = \Delta v_m (1 - \lambda_v(\nu_m)^t \beta(\nu_m)) \tag{35}$$

From (35), it is easy to conclude that $\delta J < 0$ when $|\lambda_v(\nu_m)| > 1$ and that a maximum decrease in cost is obtained when:

$$\nu_m = \arg \max_{\nu \in [\nu_1, \nu_f]} |\lambda_v(\nu)| \tag{36}$$

3. Additional coasting period conditions

For an additional initial coasting period of duration $d\nu_1$, the cost variation is given by:

$$\delta J \;=\; -\Delta v_1 \dot{\lambda}_v(\nu_1)^t \lambda_v(\nu_1) d\nu_1 \tag{37}$$

This condition means that adding an initial coasting arc of $dt_1 > 0$ duration may improve the cost if $\dot{\lambda}_v(\nu_1)^t \lambda_v(\nu_1) > 0$ i.e., the right derivative of the primer vector norm at ν_1 is positive. Similarly, for a final coasting arc of duration $d\nu_f$, we get:

$$\delta J \;=\; -\Delta v_f \dot{\lambda}_v(\nu_f)^t \lambda_v(\nu_f) d\nu_f \tag{38}$$

A final coast of $d\nu_f < 0$ duration will improve the cost when the left derivative of the primer vector at ν_f is negative.

These conditions may be used jointly to reduce the cost of a reference nonoptimal two-impulse trajectory but can also be generalized to multi-impulse trajectories. Consider the four-impulse trajectory of figure 2. For example, overall cost can be reduced by considering the coasting arc $[\nu_i, \nu_{i+1}]$, shown in Fig. 2 in different ways:

- Adding a new impulse at ν_m,
- Adding an initial coasting arc by shifting ν_i toward ν_m, if $\frac{d|\lambda|}{d\nu}(\nu_{i+1}) > 0$,
- Adding a final coasting arc by shifting ν_{i+1} toward ν_m, if $\frac{d|\lambda|}{d\nu}(\nu_{i+1}) < 0$,
- Replacing ν_i and ν_{i+1} by ν_m, if $\frac{d|\lambda|}{d\nu}(\nu_{i+1}) > 0$ and $\frac{d|\lambda|}{d\nu}(\nu_{i+1}) < 0$. This is equivalent to adding an initial and a final coasting arc on $[\nu_i, \nu_{i+1}]$ and an impulse at ν_m.

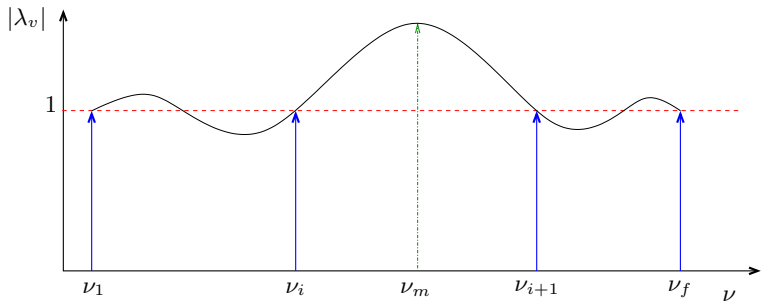

Figure 2: Adding or moving impulses on a multi-impulse trajectory

As noted in [10] and in [26], computation of the mid-impulse might nevertheless result in a nonoptimal trajectory not verifying the optimality conditions of Lawden and condition (13), particularly in the case of occurrence of a cusp at ν_m as illustrated in Fig. 3. A particular strategy combining Lion-Handelsman's conditions and local direct optimization based on the Davidon-Fletcher-Powell penalty method in [11] or based on BFGS method in [26] is generally used to optimize the resulting three-impulse trajectory.

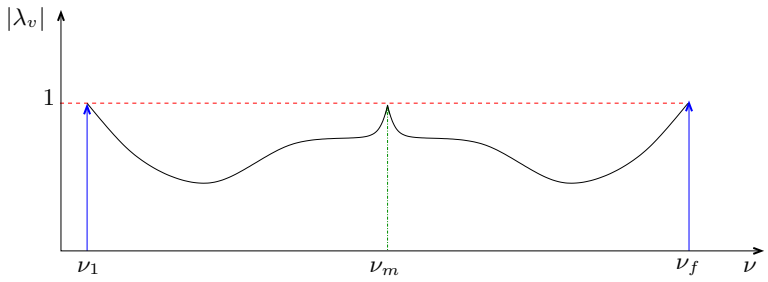

Figure 3: Nonoptimal primer vector norm with a cusp at the mid-impulse

The objective of this section is to propose an alternative to this procedure by developing a mixed iterative algorithm taking advantage of the algebraic formulation of Carter's optimality conditions and of the Lion-Handelsman's conditions.

B. A mixed iterative algorithm

Consider the following assumptions:

- The maximum number of impulses allowed is at the most equal to the Neustadt bound N_N (number of fixed state-variables in the rendezvous problem) [20]. Here, this bound is equal to 4 on the planar case and 6 for the complete rendezvous problem.

- There is an impulse at initial ν_1 and terminal ν_f dates of the fixed-time rendezvous that cannot be shifted or removed.

Based on these assumptions, improving fuel-cost will be achieved when the primer vector norm magnitude exceeds 1 at ν_m by:

- Adding impulse at ν_m if the impulse number does not exceed the upper bound N_N
- Moving impulses, if an impulse cannot be added.

The different steps of the proposed mixed algorithm are first detailed for a coplanar rendezvous $N_N = 4$ (they can easily be generalized for the general rendezvous problem $N_N = 6$) and a synoptic presentation of the algorithm is then given.

Let us first define the initialization step:

Initialization step:

a- Solve the two-impulse problem:

This problem can be solved by inverting the system of equations:

$$\begin{bmatrix} R_f \\ v_f \end{bmatrix} = \begin{bmatrix} \Phi_{11}(\nu_f,\nu_1) & \Phi_{12}(\nu_f,\nu_1) \\ \Phi_{21}(\nu_f,\nu_1) & \Phi_{22}(\nu_f,\nu_1) \end{bmatrix} \left(\begin{bmatrix} R_1 \\ v_1 \end{bmatrix} + \begin{bmatrix} 0 \\ \Delta V(\nu_1) \end{bmatrix} \right) + \begin{bmatrix} 0 \\ \Delta V(\nu_f) \end{bmatrix} \quad (39)$$

Both impulses are then given by:

$$\Delta V(\nu_1) = \Phi_{12}^{-1}(\nu_f,\nu_1)\left[R_f - \Phi_{11}(\nu_f,\nu_1)R_1 - \Phi_{12}(\nu_f,\nu_1)v_1\right] \quad (40)$$

$$\Delta V(\nu_f) = v_f - \Phi_{21}(\nu_f,\nu_1)R_1 - \Phi_{22}(\nu_f,\nu_1)v_1 - \Phi_{22}(\nu_f,\nu_1)\Delta V(\nu_1) \quad (41)$$

Initialize $T_{imp} = \{\nu_1, \nu_f\}$, where T_{imp} is the discrete set of impulses application times.

b- Compute the associated primer vector trajectory using the boundary conditions:

$$\lambda_v(\nu_1) = \frac{\Delta V(\nu_1)}{\Delta v_1} \quad (42)$$

$$\lambda_v(\nu_f) = \frac{\Delta V(\nu_f)}{\Delta v_f} \quad (43)$$

The primer vector evolution is described by:

$$\lambda_v(\nu) = \Phi_{21}^{\#}(\nu,\nu_1)\Phi_{21}^{\#-1}(\nu_f,\nu_1)\left[\lambda_v(\nu_f) - \Phi_{22}^{\#}(\nu_f,\nu_1)\lambda_v(\nu_1)\right] + \Phi_{22}^{\#}(\nu,\nu_1)\lambda_v(\nu_1) \quad (44)$$

c- Compute primer vector's maximum magnitude:

$$\lambda_m = \max_{\nu \in [\nu_1, \nu_f]} |\lambda_v(\nu)| \tag{45}$$

Iterative procedure:

1. Define $\nu_m = \arg \max_{\nu \in [\nu_1, \nu_f]} \lambda_v(\nu)$.

2. Find $\nu_a, \nu_b \in T_{imp}$ so that $\nu_a < \nu_m < \nu_b$.

3. Add a new impulse at ν_m:

$$T_{imp} \;=\; T_{imp} \cup \{\nu_m\} \tag{46}$$

4. if $dim(T_{imp}) > N_N$ then update T_{imp} according to the following cases:

   (a) If $\frac{d\lambda(\nu_a)}{d\nu}^t \lambda(\nu_a) > 0$ and $\frac{d\lambda(\nu_b)}{d\nu}^t \lambda(\nu_b) < 0$,

      (i) if $\nu_a \neq \nu_1$ then move ν_a to ν_m:

$$T_{imp} \;=\; T_{imp} - \{\nu_a\} \tag{47}$$

      (ii) if $\nu_b \neq \nu_f$ then move ν_b to ν_m:

$$T_{imp} \;=\; T_{imp} - \{\nu_b\} \tag{48}$$

   (b) If $\frac{d\lambda(\nu_a)}{d\nu}^t \lambda(\nu_a) < 0$ or $\frac{d\lambda(\nu_b)}{d\nu}^t \lambda(\nu_b) > 0$,

      (i) if $\frac{d\lambda(\nu_a)}{d\nu}^t \lambda(\nu_a) > 0$ and $\nu_a \neq \nu_1$ then move ν_a to ν_m:

$$T_{imp} \;=\; T_{imp} - \{\nu_a\} \tag{49}$$

      (ii) if $\frac{d\lambda(\nu_b)}{d\nu}^t \lambda(\nu_b) < 0$ and $\nu_b \neq \nu_f$ then move ν_b to ν_m:

$$T_{imp} \;=\; T_{imp} - \{\nu_b\} \tag{50}$$

5. Solve the polynomial multi-impulse problem using Carter's conditions on $\lambda, \Delta v_i$:

$$\lambda^t R(\nu_i) R(\nu_i)^t \lambda = 1 \quad \forall\, \nu_i \in T_{imp}$$

$$\sum_{\nu_i \in T_{imp}} \left[R(\nu_i) R^t(\nu_i)\right] \lambda \Delta v_i = -u_f$$

$$\Delta v_i \geq 0$$

6. Evaluate the new primer vector trajectory:

$$\lambda_v(\nu) \;=\; R^t(\nu)\lambda \qquad \nu \in [\nu_1, \nu_f] \tag{51}$$

7. Find primer vector's maximum magnitude:

$$\lambda_m = \max_{\nu\in[\nu_1,\nu_f]} |\lambda_v(\nu)| \tag{52}$$

Repeat "Iterative procedure" until $\lambda_m \leq 1$

Step 5 requires solving a system of polynomial equations with respect to λ and Δv_i. Note that regular algebraic tools for finding all real solutions of multivariate polynomial equations based on formal Gröbner basis computation may fail due to highly complex equations. Here, homotopy continuation methods have been used [28]. In particular, the free software package PHCPack developed by Jan Verschelde [29], [31] is used to solve the system of polynomial equations at each iteration at step 5. The systematic convergence of the algorithm for any rendezvous is not analytically proved but no such case has been reported in the different numerical tests performed so far. The algorithm is depicted in Fig. 4 flow chart.

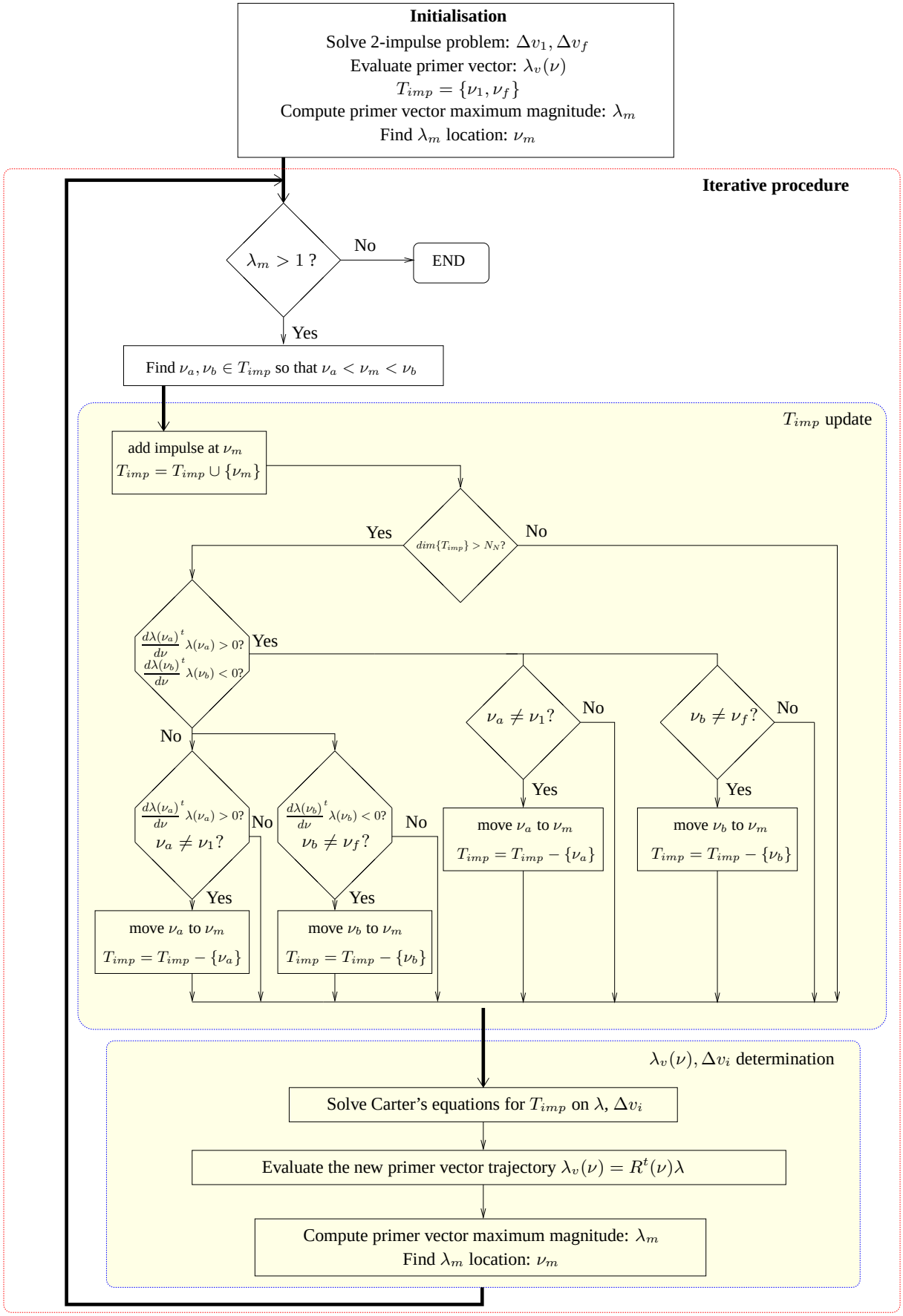

Figure 4: Iterative algorithm flowchart

V. Applications and numerical examples

In this section, numerical results obtained from the mixed iterative algorithm are compared with previous ones published in the literature [2] while global optimality is certified via the PRDV algorithm. When the mixed iterative algorithm converges to an N_{it} solution, then the PRDV algorithm certifies optimality of this solution for this fixed number of impulses while checking that there is no alternative solutions for $N = 2,\ 3,\ 4$ and $N \neq N_{it}$. Recall that the PRDV algorithm may be used to get a certificate of unfeasibility for a fixed number of impulses. Only coplanar elliptic rendezvous problems based on the Yamanaka-Ankersen transition matrix [16] are considered for numerical illustration of the results proposed. Under Keplerian assumptions and for an elliptic rendezvous, the complete rendezvous problem may be decoupled between the out-of-plane rendezvous problem for which an analytical solution may be found [7] and the coplanar problem. For the latter problem, the bound of Neustadt [20] on the optimal number of impulses is 4 and therefore $N_{max} = 4$ in the following. Note that the first two particular cases in which eccentricity $e = 0$, the Yamanaka-Ankersen transition matrix reduces to the Hill-Clohessy-Wiltshire transition matrix [30]. Finally, all numerical examples are processed using PHCpack 2.3.52 [31], [28], GloptiPoly 3.5.1 [22] and SeDuMi 1.1R3 [23] under Matlab 2008b© running on a Pentium D 3.4GHz system with 1GB ram.

A. Case study 1

Consider the numerical example given in subsection III B and borrowed from [2]. The mixed algorithm produces a four-impulse trajectory (as Carter's *a priori* solution and PRDV solution) which reduces the overall fuel consumption by finding the optimal interior impulse application times with a resolution of 5.0436 s (0.005236 rad.). The iterative algorithm reaches the optimum within 16 seconds and 8 iterations. Primer vector trajectory and impulse vectors are shown in Fig. 5 in the $(\lambda_{vx}, \lambda_{vy})$. Note that in this particular case, the upper bound on the impulse number is reached. The results obtained are compared to those presented by Carter [2] in Table 3.

	Carter [2]	Iterative Algorithm
ν_{int_1} (rad)	$\frac{\pi}{2} \simeq 1.57$	1.7017
ν_{int_2} (rad)	$\frac{3\pi}{2} \simeq 4.7124$	4.5867
$\Delta V(\nu_0)^t$	$[\ -0.0273 \quad 0.0344\ ]$	$[\ -0.02691 \quad 0.0334\ ]$
$\Delta V(\nu_1)^t$	$[\ 0.0897 \quad 0.0119\ ]$	$[\ 0.092 \quad 0.0046\ ]$
$\Delta V(\nu_2)^t$	$[\ -0.0897 \quad 0.0119\ ]$	$[\ -0.0907 \quad 0.0043\ ]$
$\Delta V(\nu_f)^t$	$[\ 0.0273 \quad 0.0344\ ]$	$[\ 0.0257 \quad 0.0318\ ]$
Fuel-cost $\mathcal{L}_1$ m/s	0.3230	0.3094
Fuel-cost $\mathcal{L}_2$ m/s	0.2688	0.2669

Table 3: Result comparison for case study 1

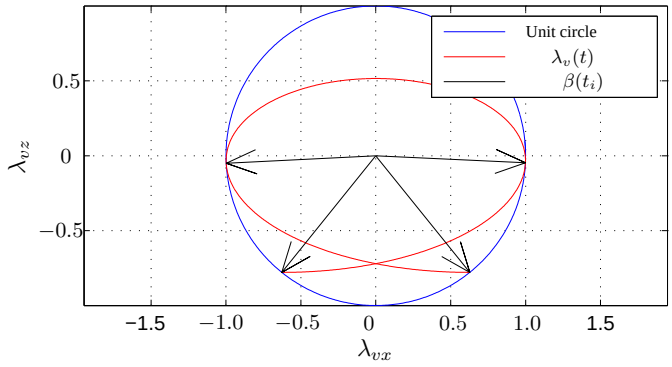

Figure 5: Primer vector in-plane trajectory for case study 1

The evolution of the primer vector norm during the iterative process is plotted in Fig. 6 where iterations associated with numerical refinements of the different solutions have been omitted.

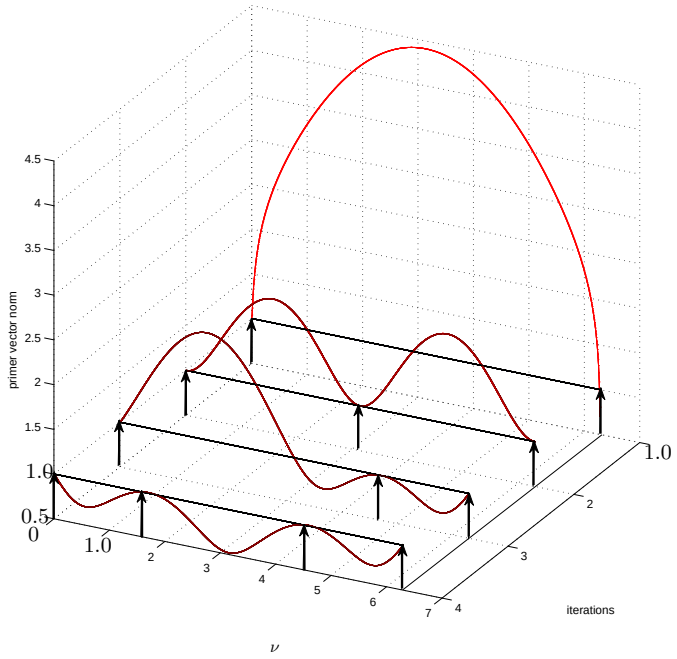

Figure 6: Norm of Primer vector during the iterative process for case study 1

The minor differences between the solutions of the iterative algorithm and that of the PRDV algorithm are mainly due to the numerical resolution chosen for both algorithms. Tighter results could be obtained at the expense of more complex numerical computations.

B. Case study 2

The second numerical illustration is a coplanar circle-to-circle rendezvous that should be completed within one orbital period and that is given in reference [2]. The chaser is one unit above the target with the same initial velocity. All characteristics are summarized in Table 4.

Eccentricity	$e = 0$
ν_0	$0\,\text{rad}$
$X_0' = [R_0'\ v_0']$	$[\,0\ \ 1\ \ 0\ \ 0\,]$
ν_f	$2\pi\,\text{rad}$
$X_f' = [R_f'\ v_f']$	$[\,0\ \ 0\ \ 0\ \ 0\,]$
N_{max}	4

Table 4: Carter's second example characteristics

The resulting optimal trajectory computed with the mixed iterative algorithm is a three-impulse rendezvous as conjectured by Carter. The primer vector trajectory plot depicted in Fig. 7 confirms the optimality of the solution for a fixed number of impulses equal to $N = 3$.

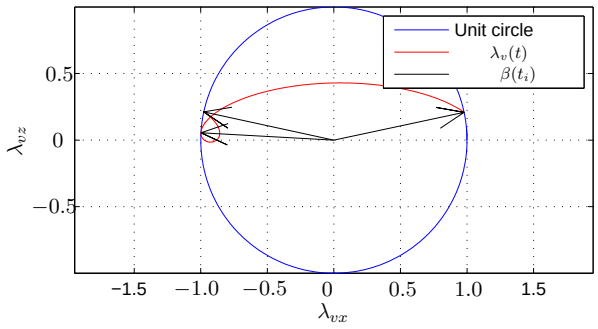

Figure 7: Primer vector in-plane trajectory for case study 2

The optimization process requires 10 iterations during 25 s. These ten steps are detailed in Figs. 8 thru 11, where each iteration is associated with one particular T_{imp} update case (see algorithm description). Note that at each step of the iterative procedure, the resulting $|\lambda_v(t)|$ function remains smooth thereby overcoming the main drawback of the usual iterative procedure originally proposed by Lion-Handelsman [9] and developed lately in [12] and [11].

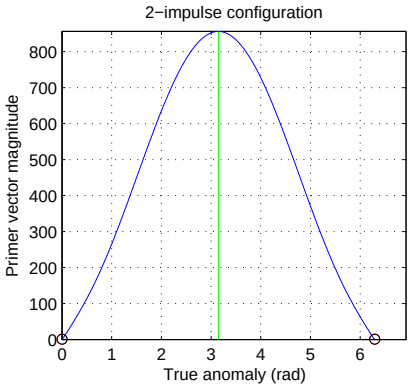

(a) Iter 1: Add impulse at $\nu = 3.146$

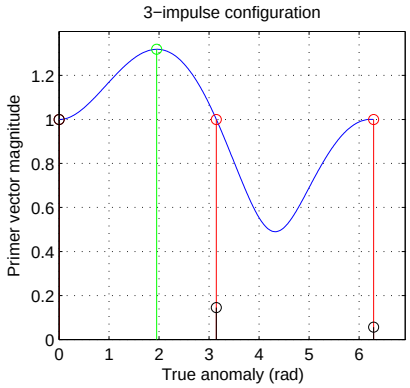

(b) Iter 2: Add impulse at $\nu = 1.950$

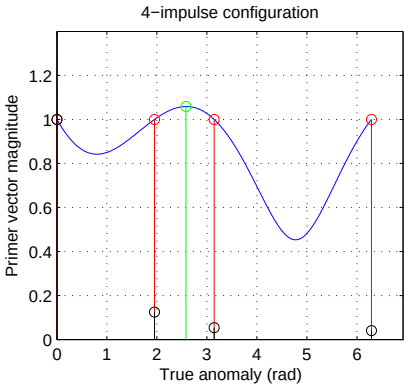

(c) Iter 3: Case (a)(i+ii)

Figure 8: Details of iterations 1-3 for case study 2

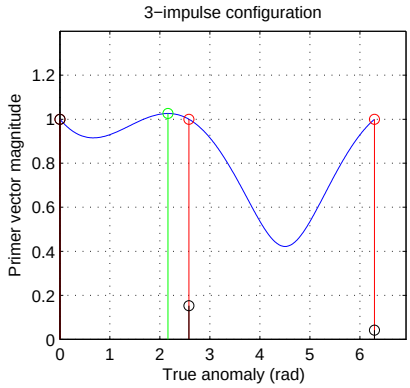

(a) Iter 4: Add impulse at $\nu = 2.559$

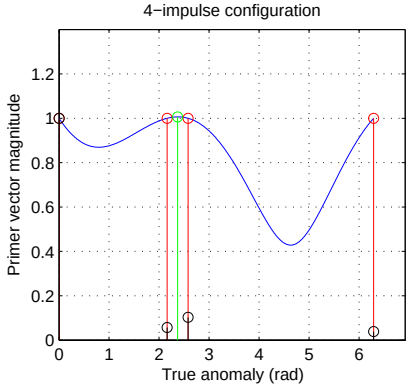

(b) Iter 5: Case (a)(i+ii)

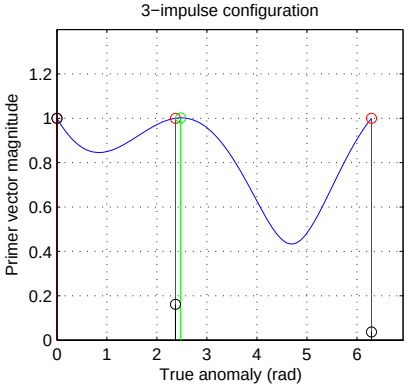

(c) Iter 6: Add impulse at $\nu = 2.475$

Figure 9: Details of iterations 4-6 for case study 2

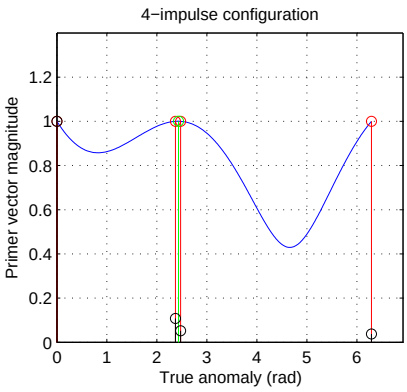

(a) Iter 7: Case (a)(i+ii)

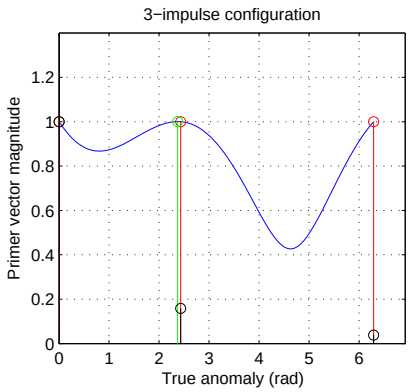

(b) Iter 8: Add impulse at $\nu = 2.370$

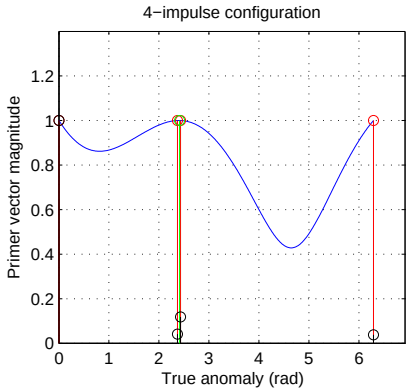

(c) Iter 9: Case (a)(i+ii)

Figure 10: Details of iterations 7-9 for case study 2

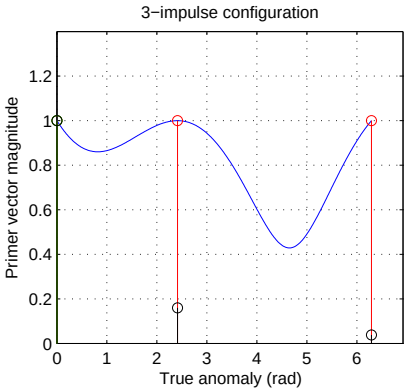

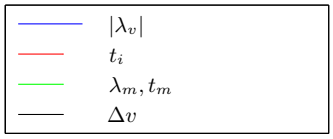

(a) Iter 10: Convergence

Figure 11: Details of iterations for case study 2

The results presented in [2] are clearly not optimal with respect to the choice of the date of application of the interior velocity increment. In [2], this location has been chosen *a priori* and it obviously results in a nonoptimal consumption as summarized in Table 5 where the results of the mixed iterative algorithm are compared to those presented by Carter in [2] with 12% fuel consumption improvement. Additionally, Table 5 lists the optimality certification furnished by the mixed iterative algorithm.

	Carter [2]	Mixed iterative Algorithm	PRDV alorithm
ν_{int} (rad)	$\frac{\pi}{2} \simeq 1.5708$	2.4119	2.4085
$\Delta V(\nu_0)^t$	$[\ 1.6294 \quad -0.6667\ ]$	$[\ 1.7775 \quad -0.3828\ ]$	$[\ 1.7771 \quad -0.38449\ ]$
$\Delta V(\nu_1)^t$	$[\ 0.3901 \quad 0.0964\ ]$	$[\ 0.2896 \quad -0.0165\ ]$	$[\ 0.28995 \quad -0.015971\ ]$
$\Delta v(\nu_f)^t$	$[\ -0.0633 \quad -0.0259\ ]$	$[\ -0.0672 \quad -0.0143\ ]$	$[\ -0.06706 \quad -0.014384\ ]$
Fuel-cost $\mathcal{L}_1$ m/s	2.8721	2.5479	2.549
Fuel-cost $\mathcal{L}_2$ m/s	2.2307	2.1770	2.1772

Table 5: Results from [2], mixed iterative and PRDV algorithms for case study 2

Figure 12 shows the in-plane trajectory of the chaser for Carter's solution (green) and mixed iterative algorithm (blue). Interestingly, the simulation of Carter's maneuver planning as proposed in [2] leads to an error at the final point of the rendezvous even with the Hill-Clohessy-Wiltshire state-transition matrix.

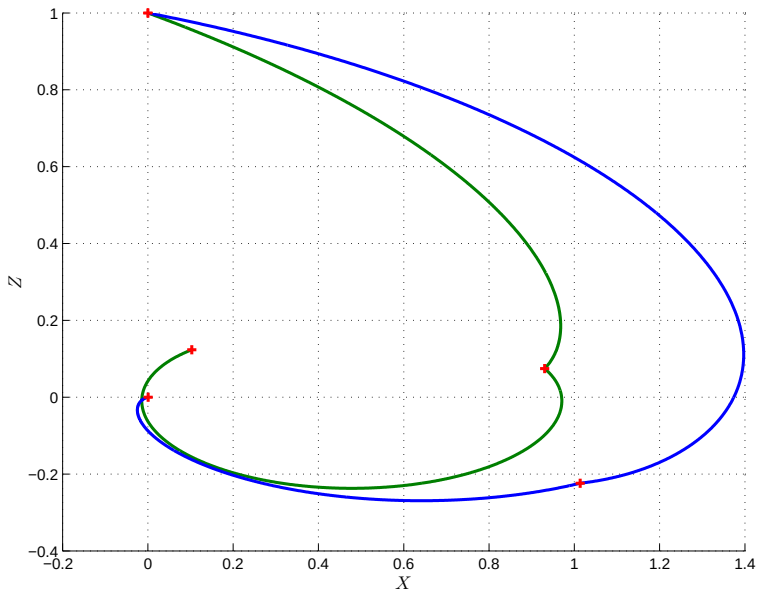

Figure 12: In-plane trajectory and impulse dates for Carter's second example: Mixed iterative algorithm (blue) and Carter's solution (green)

C. Case study 3

Following the first two academic numerical examples, a more realistic illustration based on PRISMA [17] is now presented. PRISMA programme is a cooperative effort between the Swedish National Space

Board (SNSB), the French Centre National d'Etudes Spatiales (CNES), the German Deutsche Zentrum für Luft- und Raumfahrt (DLR) and the Danish Danmarks Tekniske Universitet (DTU) [4]. Launched on June 15, 2010 Yasny (Russia), it was intended to test in-orbit new guidance schemes (particularly autonomous orbit control) for formation flying and rendezvous technologies. This mission includes the FFIORD experiment led by CNES which features a rendezvous maneuver (formation acquisition). The orbital elements of the target orbit as well as initial and final rendezvous conditions are listed in Table 6.

Semi-major axis	$a = 7011$ km
Inclination	$i = 98$ deg.
Argument of Perigee	$\omega = 0$ deg.
Right Ascension of the Ascending Node	$\Omega = 190$ deg.
Eccentricity	$e = 0.004$
True Anomaly	$\nu_0 = 0$ rad.
t_0	0 s
$X_0^t = [R_0^t \; v_0^t]$	$[\,-10 \;\; 0 \;\; 0 \;\; 0\,]$ km -km/s
t_f	64620 s
$X_f^t = [R_f^t \; v_f^t]$	$[\,-100 \;\; 0 \;\; 0 \;\; 0\,]$ m -m/s
N_{max}	4

Table 6: PRISMA rendezvous characteristics

To save fuel and allow for in-flight testing throughout the FFIORD experiment, the rendezvous maneuver must last several orbits. Duration of the rendezvous is approximately 12 hours for an expected average cost of 20 cm/s [17].

The iterative algorithm achieves optimization within 13 seconds and within 3 iterations with a chosen tolerance of 10^{-4} and a resolution of 4.8685 s (0.0052781 rad.). Global optimality of this three-impulse solution may be confirmed by running the PDRV algorithm.

	PRDV Algorithm	Iterative Algorithm
t_{int} (s)	3189.3	3198.6
ν_{int} (rad)	3.4285	3.4377
$\Delta V(\nu_0)^t$	$[\ -0.04911 \quad 0.002152\ ]$	$[\ -0.04911 \quad 0.001933\ ]$
$\Delta V(\nu_1)^t$	$[\ -0.002038 \quad 0.0000099\ ]$	$[\ -0.002039 \quad 0.0000112\ ]$
$\Delta V(\nu_f)^t$	$[\ 0.051315 \quad 0.001423\ ]$	$[\ 0.051316 \quad 0.001404\ ]$
Fuel-cost $\mathcal{L}_1$ m/s	0.10585	0.10582
Fuel-cost $\mathcal{L}_2$ m/s	0.102525	0.10252

Table 7: Results of the mixed iterative algorithm for the PRISMA case study

Figure 13 shows primer vector magnitude during transfer.

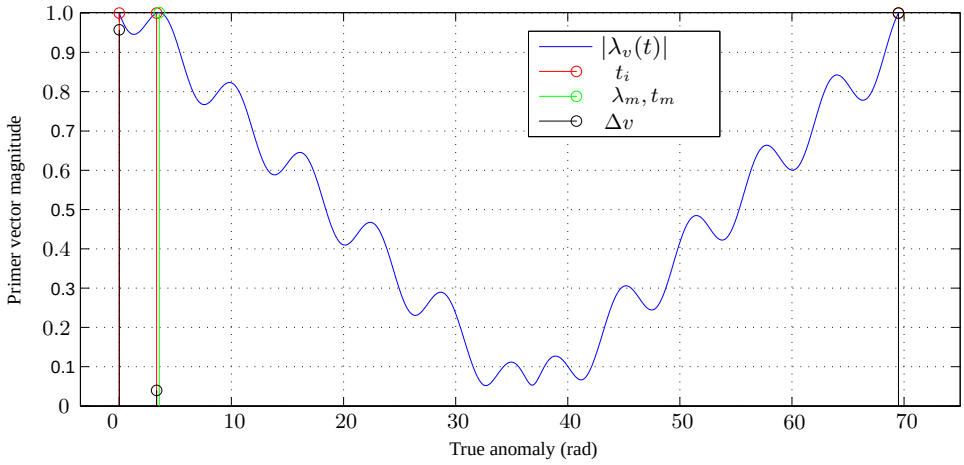

Figure 13: Primer vector magnitude during PRISMA mission

Note the low magnitude of the second impulse (0.002 m/s) with respect to the initial and final velocity increments (0.0492 m/s and 0.0513 m/s) but these velocity increments play a significant role in the optimality of the result. In particular, they provide the right chaser orientation for the long drift (61400 s) between the second impulse and the final one. Indeed, the designer could be tempted to remove this interior impulse and resort to the suboptimal two-impulse strategy. The latter solution proves to be strongly suboptimal since its $\mathcal{L}_2$ cost is $27\ \%$ greater than the optimal solution (0.14506 m/s). The long drifting period of 61400 s of the optimal solution is clearly illustrated in Fig. 14 where the in-plane trajectory and impulse positions are

represented.

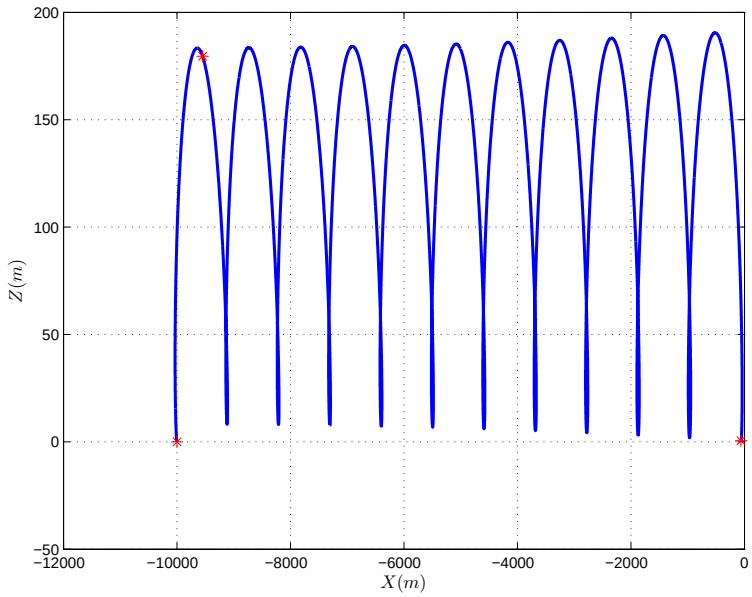

Figure 14: In-plane trajectory and impulse positions * for PRISMA mission

Finally, note that the optimal cost is half the expected average cost of 20 cm/s [17].

D. Case study 4

In order to validate both PRDV and mixed iterative algorithms for a highly elliptical reference case, the SIMBOL-X mission is now studied. SIMBOL-X is a collaborative effort between CNES (France) and ASI (Italy). It consists in a two-part high energy X-ray telescope, relying on two spacecraft. The main spacecraft orbit is highly elliptical ($e = 0.8$) with a period of 4 days. For a comprehensive description of this mission, the interested reader may consult reference [18]. The main feature of the rendezvous problem is that it is composed of two successive rendezvous maneuvers separated by a hold point. Here, we focus on the first rendezvous maneuver designed to reduce the distance from 30 km to 500 m between both satellites. The characteristics of this rendezvous are described in Table 8 where the coordinates of the initial and final relative positions and velocities are converted into the LVLH frame.

Semi-major axis	$a = 106246.9753$ km
Inclination	$i = 5.2$ deg.
Argument of Perigee	$\omega = 180$ deg.
Right Ascension of the Ascending Node	$\Omega = 90$ deg.
Eccentricity	$e = 0.798788$
True Anomaly	$\nu_0 = 135$ rad.
t_0	7 s
$X_0^t = [R_0^t \; v_0^t]$	$[\; -18309.5 \;\; 23764.7 \;\; 0.0542 \;\; 0.0418 \;]$ m -m/s
t_f	50002 s
$X_f^t = [R_f^t \; v_f^t]$	$[\; -335.12 \;\; 371.1 \;\; -0.00155 \;\; -0.00140 \;]$ m -m/s
N_{max}	4

Table 8: SIMBOL-X rendezvous characteristics

Rendezvous duration is 49995 s, that is, much shorter than the orbital period. This differs from PRISMA mission where the rendezvous lasts about 12 periods. The iterative algorithm achieves optimization within 2 seconds and 1 iteration. The final solution is a two-impulse transfer as described in Table 9.

$\begin{bmatrix} t_1 & t_f \end{bmatrix}$ (s)	$\begin{bmatrix} 7 & 50002 \end{bmatrix}$
$\begin{bmatrix} \nu_1 & \nu_f \end{bmatrix}$ (rad)	$\begin{bmatrix} 2.3562 & 2.7859 \end{bmatrix}$
$\Delta_V(\nu_1)^t$	$\begin{bmatrix} 0.6193 & -0.5061 \end{bmatrix}$
$\Delta_V(\nu_f)^t$	$\begin{bmatrix} -0.1748 & 0.4912 \end{bmatrix}$
Cost $\mathcal{L}_1$ m/s	1.7914
Cost $\mathcal{L}_2$ m/s	1.3212

Table 9: SIMBOL-X results

As shown in Fig. 15, cost cannot be improved by adding interior impulses since the primer vector norm does not exceed 1 on $[t_0, t_f]$.

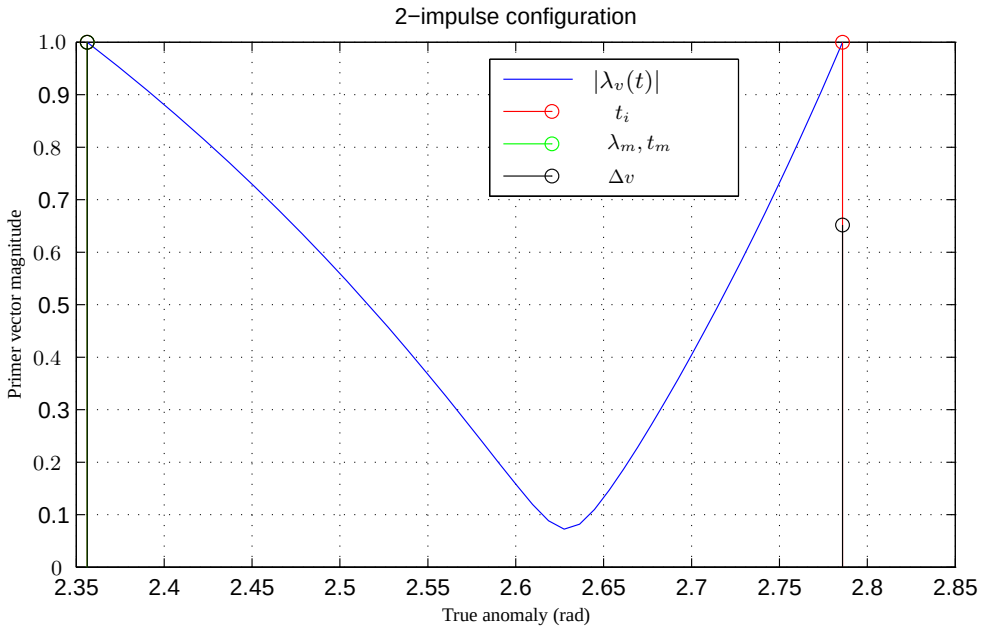

Figure 15: Primer vector magnitude for SIMBOL-X mission

Figure 16 shows the in-plane trajectory for the first rendezvous of the SIMBOL-X mission resulting in a direct transfer between chaser and target.

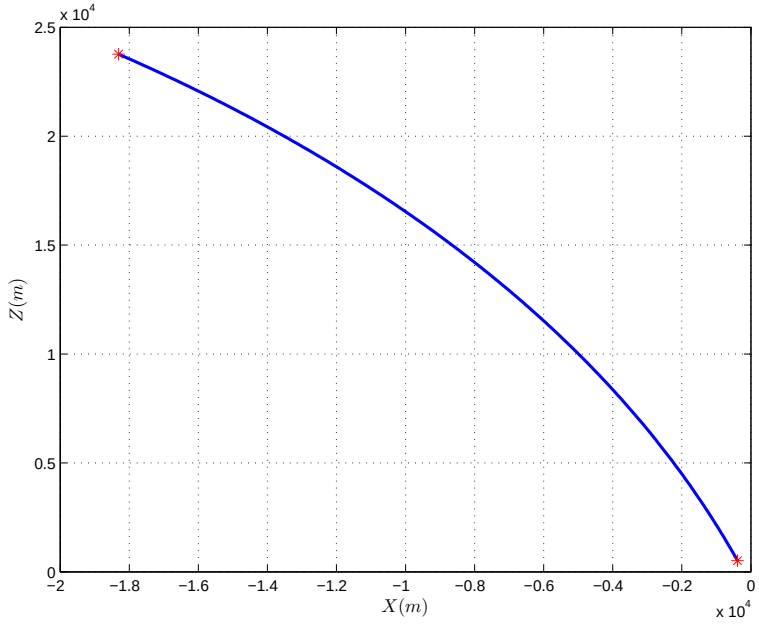

Figure 16: In-plane trajectory for the SIMBOL-X mission

The optimality of these results is also certified by running the PRDV algorithm for the 3-impulse and

4-impulse scenarios for which a certificate of unfeasibility is obtained.

VI. Conclusion

Two numerical algorithms based on polynomial optimization and tools from algebraic geometry have been proposed to address the issue of time-fixed optimal rendezvous in a linear setting. The first algorithm relying on polynomial optimization provides a guarantee of global optimality for its solution for a fixed number of impulses. The second algorithm is a mixed iterative algorithm optimizing over the number of impulses but with no guarantee of global optimality of its solution. As proposed here, both algorithms can be used jointly to get a complete solution as the first algorithm certifies the solution obtained with the mixed iterative algorithm.

Despite the good numerical results presented, some improvement can still be expected if more sophisticated transition matrices including orbital perturbation effects are used. Another avenue of research deals with the extension of previous algorithms for optimal trajectory planning with collision avoidance constraints.

Appendix

A- LVLH reference frame

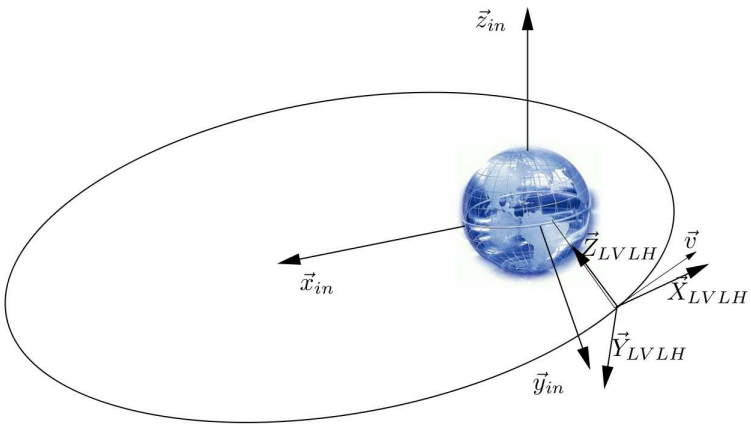

Figure 17: LVLH reference frame

The Local Vertical-Local Horizontal (LVLH) coordinate frame is a local satellite frame. It is defined as follows:

- Origin O: Target satellite center of mass

- Z axis (**R-bar**): Radial direction (Nadir-Target), oriented towards the center of the earth.
- Y axis (**H-bar**): Perpendicular to the orbital plane, points opposite the angular momentum.
- X axis (**V-bar**): Chosen such that $\vec{u_x} = \vec{u_y} \wedge \vec{u_z}$

B- Yamanaka-Ankersen transition matrix [16]

This matrix describes the in-plane relative motion of the chaser satellite, with respect to the target satellite. Assuming small distances between spacecraft and Keplerian environment, the matrix is given in LVLH reference frame:

$$\begin{bmatrix} x(t) \\ z(t) \\ v_x(t) \\ v_z(t) \end{bmatrix} = \Psi_{\nu}^{-1}\Phi_{\nu}\Phi_{\nu_0}^{-1}\Psi_{\nu_0} \begin{bmatrix} x(t_0) \\ z(t_0) \\ v_x(t_0) \\ v_z(t_0) \end{bmatrix} \tag{53}$$

where:

$\rho = 1 + e\cos\nu, \qquad k^2 = h/p^2, \qquad J = k^2(t - t_0)$

$s = \rho\sin\nu, \qquad c = \rho\cos\nu$

$s^{'} = \cos\nu + e\cos 2\nu,\ c^{'} = -(\sin\nu + e\sin 2\nu)$

$$\Phi_{\nu} = \begin{bmatrix} 1 & -c(1+1/\rho) & s(1+1/\rho) & 3\rho^2 J \\ 0 & s & c & 2 - 3esJ \\ 0 & 2s & 2c - e & 3(1 - 2esJ) \\ 0 & s^{'} & c^{'} & -3e(s^{'}J + s/\rho^2) \end{bmatrix}_{\nu} \quad \Psi_{\nu} = \begin{bmatrix} \rho I_{2\times 2} & O_{2\times 2} \\ -e\sin\nu I_{2\times 2} & (1/k^2\rho)I_{2\times 2} \end{bmatrix}_{\nu} \tag{54}$$

Aknowledgements

This work was supported by CNES Grant R-S07/VF-0001-065 and the work of fourth author was partly funded by TUBITAK.

References

[1] Prussing, J. E., and Chiu, J. H. "Optimal multiple-impulse time-fixed rendezvous between circular orbits,". *Journal of Guidance, Control and Dynamics*, Vol. 9, No. 1, Jan-Feb 1986, pp. 17-22; also AIAA paper 84-2036, Aug. 1984.

[2] Carter, T. E., "Optimal impulsive space trajectories based on linear equations," *Journal on Optimization Theory and Applications*, Vol. 70, No. 2, Aug. 1991, pp. 277-297.
doi: 10.1007/BF00940627

[3] Hughes, S. P., Mailhe, L. M., and Guzman, J. J., "A comparison of trajectory optimization methods for the impulsive minimum fuel rendezvous problem," *Advances in Guidance and Control*, edited by Ian J.Gravseth and Robert D. Culp, Vol. 113, Advances in the Astronautical Sciences, AIAA, New York, 2003, pp. 85-104.

[4] Larsson, R., Berge, S., Bodin, P., and Jonsson, U., "Fuel Efficient Relative Orbit Control Strategies for Formation Flying and Rendezvous within PRISMA," AAS 06-025, *Proceedings of the 29th Annual AAS Rocky Mountain Guidance and Control Conference*, Breckenridge, Colorado, Feb. 4-8, 2006, pp. 25-40.

[5] Lawden, D. F., "General theory of optimal rocket trajectories," *Optimal trajectories for space navigation*, 1st ed., Butterworth, London, England, 1963, pp. 54-78.

[6] Prussing, J. E., "Optimal multiple-impulse orbital rendezvous," Ph. D. Dissertation, Dept. of Aeronautics and Astronautics, Massachusetts Institute of Technology, Cambridge, MA, 1967.

[7] Prussing, J. E., "Illustration of the primer vector in time-fixed orbit transfer," *AIAA Journal*, Vol. 7, No. 6, 1969, pp. 1167-1168.
doi: 10.2514/3.5297

[8] Carter, T. E., "Necessary and sufficient conditions for optimal impulsive rendezvous with linear equations of motion," *Dynamics and control*, Vol. 10, 2000, pp. 219-227.
doi: 10.1023/A:1008376427023

[9] Lion, P. M., and Handelsman, M., "Primer vector on fixed-time impulsive trajectories," *AIAA Journal*, Vol. 6, No. 1, 1968, pp. 127-132.
doi: 10.2514/3.4452

[10] Jezewski, D. J., "Primer vector theory and applications," NASA TR R-454, Nov. 1975.

[11] Jezewski, D. J., "Primer vector theory applied to the linear relative-motion equations," *Optimal control appliactions and methods*, Vol. 1, 1980, pp. 387-401.
doi: 10.1002/oca.4660010408

[12] Jezewski, D. J., and Rozendaal, H.L., "An efficient method for calculationg optimal free-space n-impulse trajectories," *AIAA Journal*, Vol. 6, No. 11, Nov. 1968, pp. 2160-2165.
doi: 10.2514/3.4949

[13] Lasserre, J., "Global optimization with polynomials and the problem of moments," *SIAM Journal of Optimization*, Vol. 11, No. 3, 2001, pp. 796-817.
doi: 10.1.1.1.6947

[14] Parilo, P. A., "Semidefinite Programming Relaxations for Semialgebraic Problems," *Mathematical Programming, Series B*, Vol. 96, No. 2, 2003, pp. 293-320.
doi: 10.1007/s10107-003-0387-5

[15] Tschauner, J., and Hempel, P., "Rendevous zu einem in elliptischer Bahn umlaufenden Ziel," *Astronautica Acta*, Vol. II, No. 2, 1965, pp. 104-109.

[16] Yamanaka, K., and Ankersen, F., "New state transition matrix for relative motion on an arbitrary elliptical orbit," *Journal of Guidance, Control and Dynamics*, Vol. 25, No. 1, Jan-Feb 2002, pp. 60-66.
doi: 10.2514/2.4875

[17] Berges, J. C., Cayeux, P., Gaudel-Vacaresse, A., and Messygnac, B., "CNES approaching guidance experiment within FFIORD," *Proceedings of the* 21^{st} *International Symposium on Space Flight Dynamics*, Annapolis, Maryland, USA, 24-28 Sept. 2007.

[18] Gaudel, A., Berges, J. C., Trapier, T., Gamet, P., and Djalal, S., "Autonomous rendezvous guidance function of the SIMBOL-X formation flying mission a high elliptical orbit: Preliminary design and performance analysis," *Proceedings of the* 21^{st} *International Symposium on Space Flight Dynamics*, Toulouse, France, 2-5 Aug. 2010.

[19] Pereira, F. L., and Silva, G. N., "Necessary Conditions of Optimality for Vector-Valued Impulsive Control Problems," *Systems and Control Letters*, Vol. 40, 2000, pp. 205-215.
doi:10.1016/S0167-6911(00)00027-X

[20] Neustadt, L. W., "A general theory of minimum-fuel space trajectories," *SIAM Journal of Control*, Vol. 3, No. 2, 1965, pp. 317-356.

[21] Carter, T. E., and Brient, J., "Linearized impulsive rendezvous problem," *Journal of Optimization Theory and Applications*, Vol. 86, No. 3, Sept. 1995, pp. 553-584.
doi: 10.1007/BF02192159

[22] Henrion, D., and Lasserre, J. B., "Solving nonconvex optimization problems - How GloptiPoly is applied to problems in robust and nonlinear control", *IEEE Control Systems Magazine*, Vol. 24, No. 3, 2003, pp. 72-83.
doi: 10.1.1.101.2803

[23] Sturm, J. F., "Using SeDuMi 1.02, a MATLAB toolbox for optimization over symmetric cones," *Optimization Methods and Software*, Vol. 11-12, 1999, pp. 625-653.
doi: 10.1.1.49.6954

[24] Löfberg, J., "YALMIP: A Toolbox for Modeling and Optimization in MATLAB," *Proceedings of the Computer Aided Control Systems Design Conference*, Taipei, Taiwan, 4 Sep. 2004, pp. 284-289.

[25] Jezewski, D., and Donaldson, J., "An analytic approach to optimal rendezvous using Clohessy-Wiltshire equations," *Journal of the Astronautical Sciences*, Vol. 3, 1979, pp. 293-310.

[26] Guzmán, J. J., Mailhe, L. M., Schiff, C., Hughes, S. P., and Folta, D. C., "Primer vector optimization: Survey of theory, new analysis and applications," *Proceedings of the* 53^{rd} *International Astronautical Congress*, Houston, Texas, USA, 10-19 Oct. 2002.

[27] Kara-Zaitri, M. Arzelier, D., and Louembet, C., "Mixed iterative algorithm for solving impulsive time-fixed rendezvous problem," *Proceedings of the AIAA Guidance, Navigation, and Control Conference*, AIAA Paper 2010-7595, Toronto, Canada, 2-5 Aug.. 2010.

[28] Verschelde, J., "Homotopy methods for solving polynomial systems," *Proceedings of the International Symposium on Symbolic and Algebraic Computations*, Beijing, China, 2005.

[29] Sommese, A. J., and Wampler, C. W., "Homotopy Continuation," *The numerical solution of systems of polynomials*, 1st ed., World Scientific, Hackensack, NJ, 2005, pp. 15-24.

[30] Clohessy, W. H., and Wiltshire, R. S., "Terminal guidance system for satellite rendezvous," *Journal of the Aeronautical Sciences*, Vol. 27, No. 9, 1960, pp. 653-658.

[31] Verschelde, J., "Algorithm 795: PHCpack: A general-purpose solver for polynomial systems by homotopy continuation," *ACM Transactions on Mathematic Software*, Vol. 25, No. 2, 1999, pp. 251-276.